Cross-layer Goodput Analysis for Rate Adaptive IEEE 802.11a WLAN in the Generalized Nakagami Fading Channel

Li-Chun Wang, Ya-Wen Lin, and Wei-Cheng Liu
National Chiao Tung University, Taiwan, R.O.C.
Email : lichun@cc.nctu.edu.tw

***Abstract*— This paper aims to evaluate the goodput performance of the IEEE 802.11a wireless local area network (WLAN) from both the media access control (MAC) layer and physical (PHY) layer perspectives. From the physical layer perspective, we analyze the packet error rate performance of the orthogonal frequency division multiplexing (OFDM) based WLANs under the generalized Nakagami fading channel. According to the Chernoff bound analysis in the Nakagami fading channel, we derive the approximate packet error rate for the IEEE 802.11a WLAN with different data rates and fading parameters. Furthermore, we propose an efficient channel driven rate adaptation (CDRA) scheme. Through a PHY/MAC cross-layer analysis, we demonstrate that the goodput of the CDRA scheme indeed approaches to that of the optimal dynamic programming based rate adaptation method, while avoiding the complex calculations in selecting transmission parameters as the optimal method.**

I. Introduction

The IEEE 802.11a WLAN is becoming an important standard for wireless data networks because of its capability of deliver higher transmission rates compared to the first generation IEEE 802.11b WLAN. The IEEE 802.11a WLAN adopts orthogonal frequency division multiplexing (OFDM) and other advanced transmission techniques to achieve data rates ranged from 6 Mbps to 54 Mbps [1].

This paper includes two major contributions. First, we improve the analytical model of [2] to incorporate the generalized Nakagami fading channel [3]. Thus, the goodput performance of the IEEE 802.11a WLAN can be evaluated for different fading environments. Secondly, we propose a channel-driven rate adaptation (CDRA) algorithm, which can switch the PHY mode according to the available channel state information. We will show that the goodput performance of the proposed scheme approaches to that of the optimum scheme of [2].

The rest of this paper is organized as follows. Section II introduces the backgrounds for the IEEE 802.11a physical layer parameters as well as the generalized channel model. Section III develops a cross-layer goodput analysis for the rate adaptive IEEE 802.11a WLAN on the generalized Nakagami fading channel. Section IV describes our new rate adaptation scheme. Section V shows the numerical results. Finally, we conclude this paper in Section VI.

[1]This work was supported jointly by the National Science Council, Taiwan, R.O.C. under the contract 89E-FA06-2-4, EX-91EFA06-4-4, and 92-2219E009-026.

TABLE I
EIGHT PHY MODES OF IEEE 802.11A PHY

Mode	Data rate (Mbits/s)	Modulation	Bytes per Symbol, BpS	Coding rate, R
1	6	BPSK	3	1/2
2	9	BPSK	4.5	3/4
3	12	QPSK	6	1/2
4	18	QPSK	9	3/4
5	24	16-QAM	12	1/2
6	36	16-QAM	18	3/4
7	48	64-QAM	24	2/3
8	54	64-QAM	27	3/4

II. System Model and Problem Formulation

A. IEEE 802.11a Physical Layer

The IEEE 802.11a WLAN provides eight PHY modes with data rates ranged from 6 Mbps to 54 Mbps, as shown in Table I. Selecting one out of these available transmission rates will result in different goodput performances.

B. Generalized Fading Channels

In this paper, we consider the generalized Nakagami fading channel model [3]. A Nakagami-m distribution can characterize channels with different fading depths through the amount of fading (AF). Specifically, AF is defined as the ratio of the variance of the received energy to the square of the average received energy [4], i.e.

$$AF = \frac{var(A^2)}{(E[A^2])^2}, \tag{1}$$

where A is the fading amplitude. For the Nakagami-m fading model, the probability density function (pdf) of the signal amplitude is given by

$$p(A) = \frac{2m^m A^{2m-1}}{\Omega^m \Gamma(m)} \exp(-\frac{mA^2}{\Omega}), \tag{2}$$

where m is the Nakagami-m fading parameter, and Ω is the average signal power. It can be shown that in the Nakagami fading channel,

$$AF = \frac{1}{m}, \qquad m \geq \frac{1}{2}. \tag{3}$$

As $m = 1$, the Nakagami channel model becomes the Rayleigh fading channel, while as $m \to \infty$, the Nakagami-m fading channel converges to the non-faded AWGN channel. A Rician fading channel with parameter K can also be approximated by the Nakagami-m fading signal with [5]

$$K = \frac{\sqrt{m^2 - m}}{m - \sqrt{m^2 - m}}, \tag{4}$$

where K is the ratio of the power of the specular component to the scattering power.

III. Goodput Analysis Under Generalized Fading Channels

Now we want to extend the goodput analysis of [2] to the Nakagami fading channel. To achieve this objective, there are two steps. First, we need to calculate the $P_b^{(M)}$ in the formula of the first-event error probability [7]:

$$P_u^{\tilde{m}}(s) \approx \frac{1}{k} b_{d_{free}} [2\sqrt{P_b^{(M)}(s)(1 - P_b^{(M)}(s))}]^{d_{free}} \tag{5}$$

with respect to the Nakagami channel. Second, the conditional channel state transition probability $f_{R|\hat{S}}(r|\hat{s})$ is required to be recalculated with respect to the Nakagami channel model. Consider a fading channel model, where $u(t)$ is the complex envelope of input signal, $a(t)$ is the complex Gaussian random process with variance $\sigma_a^2 = 1$, and $n(t)$ is the AWGN [8]. Then the received signal $z(t)$ can be expressed as

$$z(t) = A(t)e^{j\theta(t)}u(t) + n(t) \ , \tag{6}$$

where

$$A(t) = |\gamma e^{j\psi} + a(t)| \tag{7}$$

and

$$\theta(t) = \arg[\gamma e^{j\psi} + a(t)] \ . \tag{8}$$

Note that the amplitude γ is a fixed deterministic quantity; the phase ψ is uniformly distributed over $[-\pi, \pi]$; and the envelop process $A(t)$ possesses the Rician distribution.

Assume that the fading amplitude is constant at the value A throughout a specified signaling interval, and the phase error ϕ is also a constant in the tracking loop, then the conditional bit error probability given both the value ϕ and A is [9]

$$P_b(\phi, A) = P_b^{(M)}(s \cdot A^2 \cos^2 \phi). \tag{9}$$

Thus, the bit error probability can be computed from

$$P_b = \int_0^\infty \int_{-\pi}^{\pi} P_b(\phi, A) p(\phi|A) f(A) d\phi dA, \tag{10}$$

where $p(\phi|A)$ is the conditional pdf of the phase tracking error given the fading amplitude A [10], [11]:

$$p(\phi|A) = \frac{\exp(A\alpha_0 \cos\phi)}{2\pi I_0(A\alpha_0)} \qquad -\pi \le \phi \le \pi. \tag{11}$$

In (11), α_0 is the nominal loop SNR, which exist in the absence of signal fading. Let

$$y = \frac{A^2}{\sigma_a^2} = (1 + K)A^2, \tag{12}$$

TABLE II
Required E_b/N_0 for PER = 10^{-1} under Rayleigh fading channel.

Data rate (Mbits/s)	6	9	12	18
E_b/N_0 (dB)	13.962	56.398	13.962	56.398
Data rate (Mbits/s)	24	36	48	54
E_b/N_0 (dB)	16.471	45.757	25.984	63.807

where K is the ratio of specular to diffuse energy mentioned above as (4). Then we can have

$$\begin{aligned} P_b &= \frac{1}{2\pi} \int_0^\infty \int_{-\pi}^{\pi} P_b(\phi, A) \frac{e^{A\alpha_0 \cos\phi}}{I_0(A\alpha_0)} \\ &\quad \frac{2A}{\sigma_a^2} e^{\frac{-(A^2+\gamma^2)}{\sigma_a^2}} I_0(\frac{2A\gamma}{\sigma_a^2}) d\phi dA \\ &= \frac{e^{-K}}{2\pi} \int_0^\infty \int_{-\pi}^{\pi} P_b(\phi, \sqrt{\frac{y}{1+K}}) \\ &\quad \frac{e^{\sqrt{\frac{y}{1+K}}\alpha_0 \cos\phi}}{I_0(\sqrt{\frac{y}{1+K}}\alpha_0)} e^{-y} I_0(2\sqrt{yK}) d\phi dy. \end{aligned} \tag{13}$$

The analysis and simulation results for the error performances over the generalized fading channel will be compared in Section V. From (refeq:PbQRi), we can analyze the effective goodput and derive the SNR boundary in our CDRA scheme, which will be discussed in detail in the next section.

IV. Link Adaptation Scheme

A. Algorithm

In this paper, we propose a channel-driven rate adaptation (CDRA) algorithm to take account of channel conditions when selecting physical transmission parameters. Specifically, CDRA algorithm switches to the best PHY mode (i.e. modulation and coding scheme) as soon as the channel state information is available. The algorithm is detailed as follows:

1) Set the required PER.
2) Calculate the PER of these eight PHY modes under the interested channels.
3) Find the required E_b/N_0 for each PHY mode using interpolation.
4) Observe the required E_b/N_0s for each PHY mode, pick the efficient modes at E_b/N_0 boundaries of channel state s_i, η_{i-1} and η_i, for i from 1 to N.
5) Map the channel state to s_i and switch the system to the corresponding PHY mode at the instant of every retry.

B. Reduced Mode Rate Adaptation

From (26) of [2] and (5), we can calculate the PER for AWGN, Rayleigh fading, and Rician fading channels. Here we first consider Rayleigh fading channel, i.e., the case of m=1 in Nakagami fading channel. Let the required PER as 0.1. By computing the PERs of some E_b/N_0, we can get the required E_b/N_0 for each PHY mode, as shown in Table II.

From the table, we can see that the PHY modes with data rates equal to 6 and 12 Mbps have the same performance,

which implies that the 6 Mbps PHY mode is not needed. Similarly, because 9 and 18 Mbps modes have the same performance, the 9 Mbps mode is not needed. Moreover, because the required E_b/N_0 for 24 Mbps is smaller than that of 18 Mbps, the receiver does not need the 18 Mbps mode. Note that the required E_b/N_0 of 48 Mbps is smaller than that of 36 Mbps. Consequently, 36 Mbps mode can be removed. Now, we just use 12, 24, 48, and 54 Mbps modes. The boundaries of selecting these regions are: $\eta_1 = 16.471$ dB, $\eta_2 = 25.984$ dB, and $\eta_3 = 63.807$ dB.

C. Generalized Nakagami-m Fading Channel Model

Let x_i and x_{i+1} represent the SNR values at the i-th and $(i+1)$-th retry, respectively. Then we can express p_{jk} as :

$$\begin{aligned} p_{jk} &= P(x_{i+1} \in (\eta_{k-1}, \eta_k) | x_i \in (\eta_{j-1}, \eta_j)) \\ &= \frac{P(x_{i+1} \in (\eta_{k-1}, \eta_k), x_i \in (\eta_{j-1}, \eta_j))}{P(x_i \in (\eta_{j-1}, \eta_j)}. \end{aligned} \quad (14)$$

Now we calculate the joint pdf $p(x_i, x_{i+1})$ in order to obtain $P(x_{i+1} \in (\eta_{k-1}, \eta_k), x_i \in (\eta_{j-1}, \eta_j))$.

Denote $\alpha_{t-\tau}$ and α_t as the channel fades at time instants $t-\tau$ and t, respectively. In the Nakagami fading channel, the joint pdf $p(\alpha_{t-\tau}, \alpha_t)$ is given by [3]

$$\begin{aligned} p(\alpha_{t-\tau}, \alpha_t) &= \frac{4(\alpha_{t-\tau}\alpha_t)^m}{(1-\rho)\Gamma(m)\rho^{(m-1)/2}} \left(\frac{m}{\Omega}\right)^{m+1} \\ & I_{m-1}\left(\frac{2m\sqrt{\rho}\alpha_{t-\tau}\alpha_t}{(1-\rho)\Omega}\right) \\ & \exp\left(-\frac{m(\alpha_{t-\tau}^2 + \alpha_t^2)}{(1-\rho)\Omega}\right), \end{aligned} \quad (15)$$

where $I_{m-1}(.)$ is the $(m-1)^{th}$-order modified Bessel function of the first kind, $\Gamma(m)$ is the Gamma function, m is the Nakagami fading parameter, and $E[\alpha_{t-\tau}^2] = E[\alpha_t^2] = \Omega$. Note that Ω is normalized to 1 in this paper. From [6], the channel correlation coefficient ρ in (15) can be expressed as

$$\rho = \frac{J_0(2\pi f_d \tau) + K\cos(2\pi f_d \tau \cos\theta_0)}{2+2K}, \quad (16)$$

where K is the ratio of the specular power to scattered power, the θ_0 is the angle of arrival phase.

Assume that the Doppler spread $f_d = 0$ Hz, i.e., no relative movement between the transmitter and the receiver. Then $\rho = 0.5$. Thus, we have

$$\begin{aligned} & P(x_{i+1} \in (\eta_{k-1}, \eta_k), x_i \in (\eta_{j-1}, \eta_j)) \\ = & \int_{\eta_{k-1}}^{\eta_k} \int_{\eta_{j-1}}^{\eta_j} p(\alpha_{t-\tau}, \alpha_t) d\alpha_{t-\tau} d\alpha_t \end{aligned} \quad (17)$$

and

$$\begin{aligned} & P(x_i \in (\eta_{j-1}, \eta_j)) \\ = & \int_0^{\infty} \int_{\eta_{j-1}}^{\eta_j} p(\alpha_{t-\tau}, \alpha_t) d\alpha_{t-\tau} d\alpha_t. \end{aligned} \quad (18)$$

Substituting (14) into (17) and (18), we can get all N^2 transition probabilities, p_{jk}, where $j, k = 1, \ldots, N$. After obtaining the transition probabilities, we can apply them to calculate goodput with the E_b/N_0 transition threshold in our proposed rate adaptation scheme. The approach of calculating the transition probabilities can be used for both the complete and the reduced modes. Once we know the number of channel states and the E_b/N_0 values of decision boundaries, we can calculate the transition probabilities of the channel with any states.

D. Goodput Computation

The goodput computation of CDRA scheme is similar to the method described in [2]. However, it can be further simplified. As we know the E_b/N_0 value of transmission, we can choose the PHY mode. Note that $f_{R|S}(r|s)$ can be replaced by p_{jk} to indicate the case $s \in (\eta_{j-1}, \eta_j)$ and $r \in (\eta_{k-1}, \eta_k)$, and $\tilde{m}$ is a function of the channel state. Then $E[data]$ can be simplified as:

$$\begin{aligned} & E[data](\ell, s, \tilde{m}, n) \\ = & P_{s,xmit}(\ell, s, \tilde{m}) \cdot \ell + [1 - P_{s,xmit}(\ell, s, \tilde{m})] \\ & \cdot \sum_{k=1}^{N} p_{jk} \cdot E[data](\ell, r, \tilde{m}(r), n+1), \end{aligned} \quad (19)$$

where N is the number of channel state. Now $E[\mathcal{D}_{data}]$ can be simplified as

$$\begin{aligned} & E[\mathcal{D}_{data}](\ell, s, \tilde{m}, n) \\ = & \overline{T}_{bkoff}(n) + T_{data}(\ell, \tilde{m}) + tSIFSTime + T_{ack}(\tilde{m}) \\ & + P_{s,xmit}(\ell, s, \tilde{m}) \cdot tDIFSTime + [1 - P_{s,xmit}(\ell, s, \tilde{m})] \\ & \cdot \left\{ \overline{\mathcal{D}}_{wait}(n+1) + \sum_{k=1}^{N} p_{jk} \cdot E[\mathcal{D}_{data}](\ell, r, \tilde{m}(r), n+1). \right\} \end{aligned} \quad (20)$$

Substituting (14) into (19) and (20), we can easily get the goodput performance of our CDRA scheme.

V. Numerical Results

A. Effect of Fading Channel on Packet Error Probability Performance

In Fig. 2, we can see that because (5) is actually the Chernoff bound, the PER performance by simulation are bounded by the analytical values obtained from (5). The E_b/N_0 difference between the analytical approximation and simulation is about 1 dB, 2 dB, and 3 dB for the PHY modes 3, 5, and 7, respectively. The differences result from the fact that the combination of (24) in [2] and the bound of the first-event error probability of hard-decision Viterbi decoder in (5) is just an approximation. As the modulation level increases, the differences between the approximate packet error rate and the simulation value results becomes more significant.

Figure 3 shows the error rate performances of the IEEE 802.11a WLAN over the Rayleigh fading channel. The PER performances by analysis converge faster than those by simulation. As the E_b/N_0 value increases, the simulation and analysis results get closer . Figure 4 compares the analytical and simulation error performances over the Nakagami channel

TABLE III

LINK BUDGET ANALYSIS OF GOODPUT USING CDRA SCHEME IN DIFFERENT CHANNELS

Goodput	d=2m	d=5m	d=10m	d=25m	d=50m
Rayleigh	28.093	23.859	14.624	0.28464	2.7653×10^{-5}
Rician	30.947	30.905	26.986	8.0188	1.0492
AWGN	31.027	30.524	21.915	7.4811	2.9054

TABLE IV

LINK BUDGET ANALYSIS OF GOODPUT USING MPDU-BASED LINK ADAPTATION SCHEME IN DIFFERENT CHANNELS

Goodput	d=2m	d=5m	d=10m	d=25m	d=50m
Rayleigh	28.382	25.182	14.853	0.28485	2.7653×10^{-5}
Rician	30.947	30.91	27.233	8.0809	1.2448
AWGN	31.027	30.471	22.273	8.2527	4.9395

with m=5. As the E_b/N_0 value increases, the simulation and analysis results approach to the same values. For PER= 10^{-1}, the E_b/N_0 values of analytical approximation and simulation are almost the same.

From Figs. 2 to 4, we can see that in both Rayleigh and Rician fading channels, the analysis and simulation of error performances are very close for PER smaller than 10^{-1}. Thus we can ensure that the decision boundaries for the rate adaptation scheme can be chosen from the proposed analytical approximation method, i.e. according to (26) in [2], (5), (24) in [2], and (13). Comparing Figs. 5, 6, and 7, we can find that for large E_b/N_0, the goodput performances of Rician fading channels and AWGN channel are very close to 31 Mbps. On the contrary, as E_b/N_0 is small, the goodput performances of both the rate adaptation schemes in the AWGN channel is better than that in the Rician fading channel.From the figures, we can conclude that our proposed CDRA scheme performs closely to the "optimum" dynamic programming link adaptation scheme, while it is simpler and easy to be implemented. Moreover, we can observe that because of the overhead of the time slots required for detection, training symbol, etc., the MAC layer goodput performance is hard to reach the predefined physical layer data rate. For example, the goodput performance of E_b/N_0 equal to 29 dB never reach the value of 54 Mbps even in the PHY mode 8.

B. Average Goodput Performance with Link Budget Analysis

Tables III, IV, and V show the goodput in Mbps for the CDRA scheme, MPDU-based link adaptation scheme, and single-mode link adaptation scheme, respectively. From these three tables, we can see that if the distance between the transmitter and receiver is short, the goodput performance of Rician fading channel is close to AWGN channel. As the distance increases, the goodput performance of Rician fading channel decays faster than that in the AWGN channel. Comparing the data in the three tables for different channels, we can find that the proposed CDRA scheme is only slightly worse than the dynamic programming approach. Hence, we can conclude that the proposed CDRA scheme possesses the features of computation efficiency and high goodput performance.

TABLE V

LINK BUDGET ANALYSIS OF GOODPUT USING SINGLE-MODE LINK ADAPTATION SCHEME IN DIFFERENT CHANNELS

Goodput	d=2m	d=5m	d=10m	d=25m	d=50m
Rayleigh	17.794	13.877	10.141	0.05253	1.0186×10^{-11}
Rician	28.805	28.707	16.808	5.0784	0.98057
AWGN	28.887	26.627	13.993	2.7856	2.6712

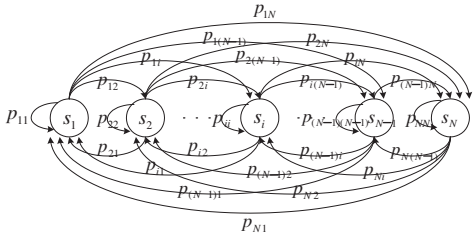

Fig. 1. An N-state generalized Nakagami fading channel model.

VI. CONCLUSIONS

In this paper, we have developed a cross-layer analytical model to calculate the MAC protocol efficiency of IEEE 802.11 WLAN under the Nakagami fading channel. Furthermore, we have proposed an efficient channel-driven rate adaptation (CDRA) scheme. In Section V, we show that the CDRA scheme is simple and efficient, while achieving almost the same performance as the optimum dynamic programming link adaptation scheme. Because the E_b/N_0 decision boundary is determined analytically, we can easily provide the E_b/N_0 regions for any channels without time-consuming simulation.

REFERENCES

[1] IEEE 802.11a, *Part 11: wireless LAN Medium Access Control (MAC) and Physical Layer (PHY) specifications: High-speed physical layer in the 5 GHz band,* Supplement to IEEE standard for information technology telecommunications and information exchange between systems - local and metropolitan area networks - specific requirements, 1999.

[2] Daji Qiao, Sunghyun Choi, and K.G. Shin, "Goodput analysis and link adaptation for IEEE 802.11a wireless LANs," *IEEE Transactions on Mobile Computing*, vol. 1, no. 4, pp. 278-292, Oct.-Dec. 2002.

[3] M. Nakagami, *Statistical Methods in Radio Wave Propagation*. Pergamon Press, Oxford, U.K., 1960.

[4] U. Charash, "Reception through Nakagami fading multipath channels with random delays," *IEEE Trans. Commun.*, vol. 27, pp. 657-670, Apr. 1979.

[5] Gordon L. Stüber, *Princicples of Mobile Communication*, Second Edition, Kluwer Academic Publishers, 2001.

[6] Chengshan Xiao and Y.R. Zheng, "A statistical simulation model for mobile radio fading channels," *IEEE Wireless Communications and Networking Conference*, vol. 1, pp. 144-149, 16-20 Mar. 2003.

[7] S. B. Wicker, *Error Control Systems for Digital Communication and Storage*. pp. 304-314, 1st Edition, Prentice-Hall, 1995.

[8] J. Modestino and Mui Shou, "Convolutional Code Performance in the Rician Fading Channel" *IEEE Transactions on [legacy, pre - 1988] Communications*, vol. 24, no. 6, pp. 592 -606, Jun 1976.

[9] J. M. Wozencraft and I. M. Jacobs, *Principles of Communication Engineering*. New York: Wiley, 1965, ch. 7.

[10] A. J. Viterbi, *Principles of Coherent Communication*. New York: McGraw-Hill, 1966.

[11] W. C. Lindsey, *Synchronization Systems in Communication and Control*. Englewood Cliffs, NJ: Prentice-Hall, 1972.

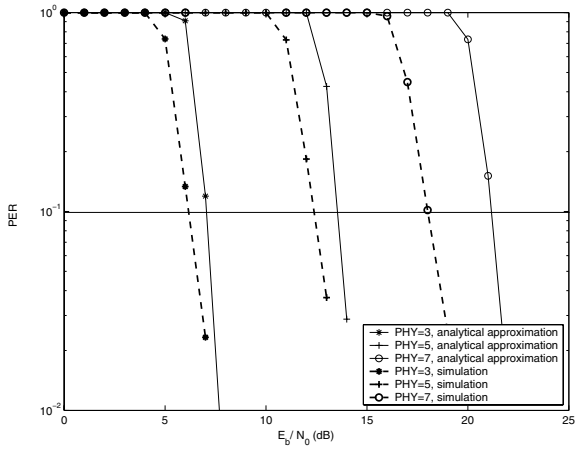

Fig. 2. The comparison between analysis and simulation for error performances in the AWGN channel.

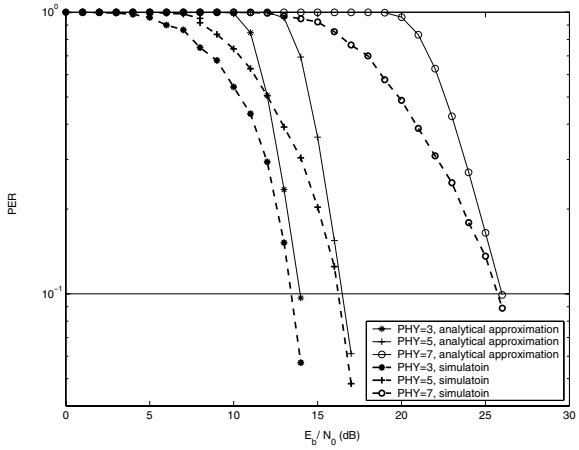

Fig. 3. The comparison between analysis and simulation for error performances in the Rayleigh fading channel (Nakagami parameter m=1).

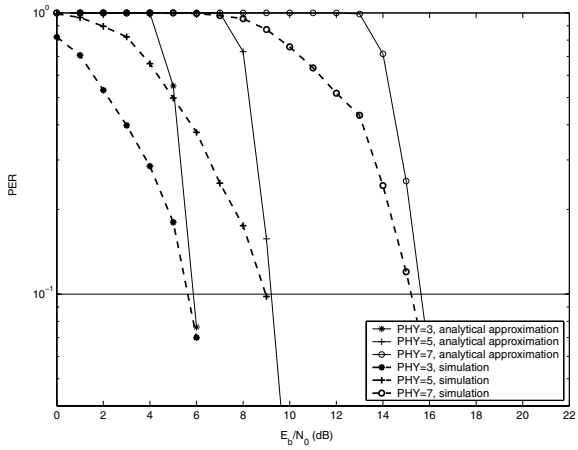

Fig. 4. The comparison between analysis and simulation of error performances in Rician Channel (Nakagami parameter m=5).

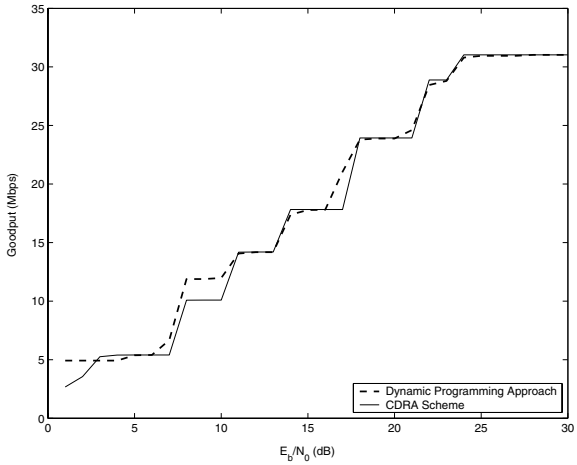

Fig. 5. Goodput performance of our CDRA scheme and the dynamic programming link adaptation scheme over the AWGN channel.

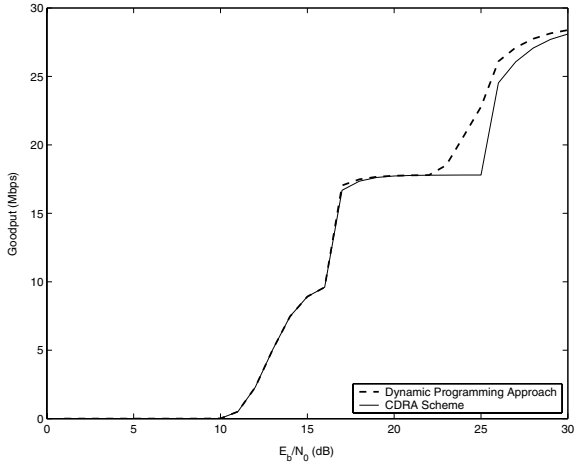

Fig. 6. Goodput performance of our CDRA scheme and the dynamic programming link adaptation scheme over Rayleigh fading channel (Nakagami parameter m=1).

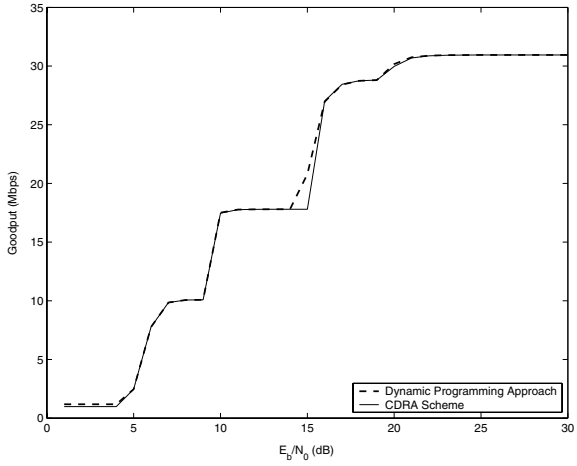

Fig. 7. Goodput performance of our CDRA scheme and the dynamic programming link adaptation scheme over Rician fading channel (Nakagami parameter m=5).